Clean Technologies and Environmental Policy (2019) 21:179–199
https://doi.org/10.1007/s10098-018-1627-y

ORIGINAL PAPER

Evaluation of riverbank filtration in the removal of pesticides: an approximation using column experiments and contaminant transport modeling

Marcela Jaramillo[1] · Thomas Grischek[2] · Hilmar Boernick[3] · Jaime I. Velez[4]

Received: 18 January 2018 / Accepted: 10 October 2018 / Published online: 17 October 2018
© Springer-Verlag GmbH Germany, part of Springer Nature 2018

Abstract

The potential of riverbank filtration in the removal of five pesticides commonly used in Colombia (atrazine, ametryn, carbofuran, diuron and propanil) was evaluated through a series of column experiments and solute transport modeling. The experiments consisted of two soil columns run under saturated regime, with sediments and water collected from the rivers Loessnitztal and Elbe (East Germany), respectively. Six experiments were performed at 10 and 20 °C, and the final concentrations of the pesticides were used to solve the one-dimensional advection–dispersion equation using an inverse approach. Variables such as retardation factor, first-order degradation coefficient, and dispersion coefficient were assessed for all the pesticides except propanil, which rapidly degraded in solution. The parameters obtained for one of the experiments were introduced into a groundwater flow model from the Loessnitztal site, and the code MT3DMS was used to simulate a contaminant pulse coming from the river. Four different scenarios were considered to determine the effect of adsorption and degradation on the fate of the pesticides. The results showed that, although the persistence of pesticides depends on the properties of each compound, a maximum of 30% removal was achieved during the column experiments, and a log removal of 9 through the numerical modeling. Because of the sensitivity of the fate of contaminants to sorption and degradation, field and laboratory work should be carried on to determine the removal coefficient of the dissolved and adsorbed phases of the compounds, the type of degradation to be expected, and the real values of longitudinal and transverse dispersivity.

✉ Marcela Jaramillo
majaram9@eafit.edu.co

Thomas Grischek
grischek@htw-dresden.de

Hilmar Boernick
hilmar.boernick@tu-dresden.de

Jaime I. Velez
jivelezu@unal.edu.co

[1] Department of Earth Sciences, Faculty of Science, EAFIT University, Cr. 49 # 7 Sur-50, Medellin, Colombia

[2] Faculty of Civil Engineering and Architecture, University of Applied Sciences Dresden (HTW Dresden), Friedrich-List-Platz 1, 01069 Dresden, Germany

[3] Institute for Water Chemistry, Technische Universität Dresden (TU-Dresden), 01069 Dresden, Germany

[4] Faculty of Mines, School of Geosciences and Environment, National University of Colombia, Cr. 80 # 65-223, Medellin, Colombia

Graphical Abstract

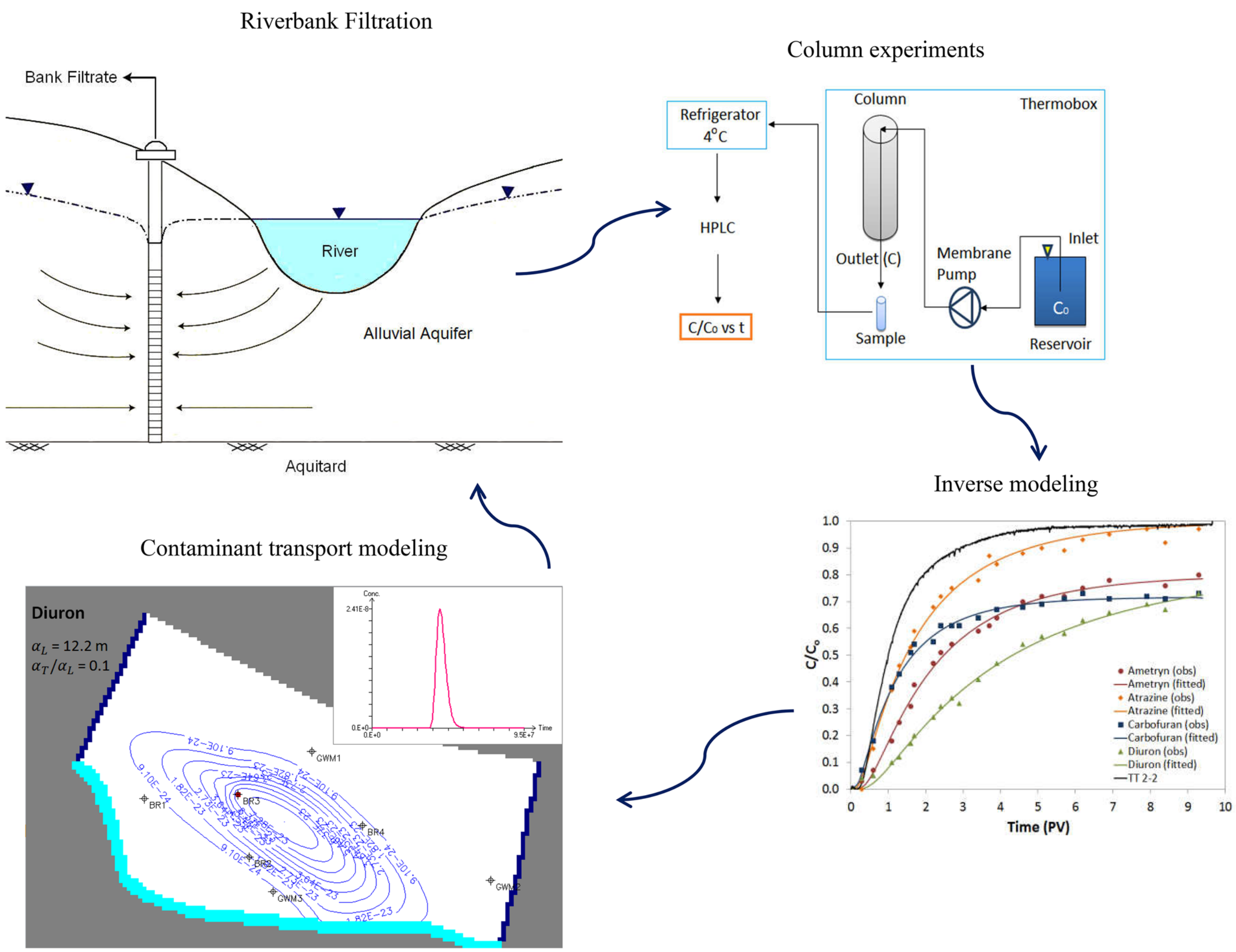

Keywords Riverbank filtration · Pesticide removal · Solute transport · Numerical modeling · Column experiment

Introduction

Pesticides are organic chemical compounds intentionally released into the environment to control, eliminate or destroy pests in agricultural corps or livestock, in order to benefit human beings (Rashid et al. 2010). However, they can also be toxic for living organisms, difficult to degrade, and persistent in the environment due to bioaccumulative effects (Ormad et al. 2008). By runoff, groundwater discharge or atmospheric deposition pesticides can reach surface water bodies, and their presence in groundwater might be attributed to either direct leaching from agricultural fields or recharge from rivers contaminated with them (Verstraeten et al. 2002a).

The fate and transport of pesticides in the subsurface depend on factors, such as: physical and chemical properties of the compounds (solubility, size, polarization, and volatility); hydrological conditions; type of soil and sediments; physical, chemical, and biological processes in the soil and in the vadose and saturated zones (Verstraeten et al. 2002a; Rashid et al. 2010). The aforementioned processes include advective transport, hydrodynamic dispersion, precipitation, sorption, volatilization, and degradation by biotic and abiotic mechanisms (Hiscock and Grischek 2002). However, sorption and biodegradation are the most dominant in determining the occurrence of pesticides in a water–sediment system (Son 2010).

Some pesticides can transform chemically, but the subproducts tend to be less toxic than their parent compounds (Sinclair and Boxall 2003). However, the transformation products represent a greater contamination threat (Baluch et al. 1993; Scribner et al. 2000) because they solubilize easier, leach more rapidly (Scribner et al. 2000), and persist longer in the environment (Verstraeten et al. 2002b).

Colombia (South America) is considered to be an agricultural country, and such activity constitutes the most common industry for internal use and export, and requires the use of agrochemicals. According to the Colombian Agricultural Institute (ICA 2016), the volume of pesticides used in the country in 2015 was about 11.8 millions of tons (solid presentation) and 41.4 millions of liters (liquid formulation), which represented a 21% increase compared to 2010 (ICA 2011). Unfortunately, the country does not have yet a system that permits to estimate the amount of pesticides discharged annually into the water bodies (IDEAM 2010), because the monitoring network includes only dissolved oxygen, total suspended solids, electric conductivity, pH, biological oxygen demand, chemical oxygen demand and, in some cases, total nitrogen and total phosphorous (IDEAM 2015).

Due to poor agricultural practices, fertilizers and pesticides (some of which can be toxins, carcinogens or teratogens) are applied in excess and, by runoff, usually end up in the surface water bodies (IAvH et al. 2011; IDEAM 2010). The quality of those water bodies is further affected by the wastewater that is discharged into them–only 15% of the country's wastewater is somehow treated before its release into the environment (Defensoria del Pueblo 2010).

Considering that in Colombia most drinking water treatment plants obtained the water from surface sources, it comes as no surprise that in the second semester of 2009 almost 70% of the cities received water that was unsafe for human consumption, i.e., when the water quality meets less than 95% of the standards established in the Colombian legislation (Defensoria del Pueblo 2010). Besides the quality of the water sources, other possible causes for the poor drinking water quality are related to the drinking water treatment plants (Defensoría del Pueblo 2007): (1) complete absence of them; (2) very basic procedures or without the specific technical regulations; (3) inadequate operation and low technical knowledge of the people operating them; (4) problems in distribution networks, which are inefficient and obsolete; (5) scarce financial resources destined to build/update them.

It is therefore necessary to evaluate alternatives that allow the Colombian population to have access to water of adequate quality, thus reducing the risks to public health, and the treatment and maintenance costs. In this regard, the use of riverbank filtration, or exploitation of alluvial aquifers hydraulically connected to surface water, has advantages such as high production potential, ease and economy of extraction (Doussan et al. 1997).

Riverbank filtration (RBF) is a drinking water treatment technology that uses the aquifer as a natural filter (mechanical, biological and chemical) in order to reduce the concentration of pollutants in the surface water source (Tufenkji et al. 2002). Several authors have investigated the potential of RBF in the removal of specific pesticides and report that some of them show complete removal (Son 2010), while others cannot be fully eliminated and additional treatment techniques might be needed to remove byproducts and parent compounds (Verstraeten and Heberer 2002). Regardless, the concentration of organic compounds in bank filtrate has been reported to be lower than in the river water (Schaffner et al. 1987; Ray et al. 1998; Verstraeten et al. 1999; Kuehn and Mueller 2000).

For more information on the presence of pesticides in the environment, the adverse effects of these compounds on the ecosystem and human health, and some particular experiences with RBF in the removal of organic pollutants, the reader is encouraged to refer, respectively, to the comprehensive works of Buchanan et al. (2010), Rashid et al. (2010), and Verstraeten et al. (2002a).

Although RBF has been used for more than a century in Europe and half a century in the US, the current understanding of the processes and mechanisms behind the technique are still very empirical (Tufenkji et al. 2002), and because the efficiency of RBF depends on specific site conditions (hydraulics, hydrogeology and hydrochemistry), it is difficult to define general guidelines on the conditions necessary for the protection and optimization of RBF sites (Hiscock and Grischek 2002). The completion of more studies on the performance of RBF under a wide range of environmental conditions may improve the design, operation, and monitoring of RBF systems (Tufenkji et al. 2002).

In order to determine the fate of agrochemicals during RBF, five active ingredients were selected for laboratory experiments and contaminant transport modeling. The pesticides chosen—ametryn, atrazine, carbofuran, diuron, and propanil—are of common use in Colombia (ICA 2016), even though the EPA in the USA and the European Union in Europe have either prohibited or banned all of them, except diuron (SAN 2011).

The main goal of this paper is to present the most relevant results from the column experiments and the numerical modeling and contribute to determining the potential of riverbank filtration to remove these pesticides from river water, and also the possibility of using the technology as a drinking water treatment alternative in Colombia, where RBF is almost completely unknown (Jaramillo 2012). To the best of our knowledge, few studies have been undertaken to establish the fate of the contaminants considered here during RBF. Atrazine has been studied more than any of the other pesticides (Benotti et al. 2012; Bertelkamp et al. 2014, 2016; Kuster et al. 2010; Ray et al. 2002; Verstraeten et al. 2002b), followed by diuron (Sánchez-Pérez et al. 2013; Kuster et al. 2010; Bertelkamp et al. 2016), carbofuran (Romero et al. 2010), and no study has consider ametryn.

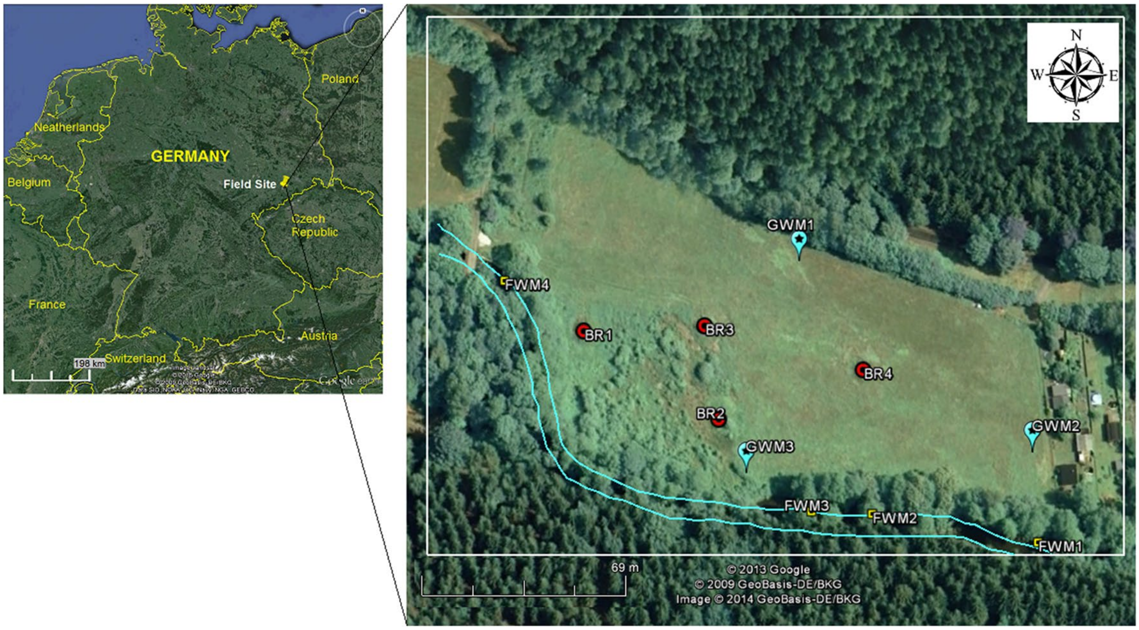

Fig. 1 Study area in Loessnitztal, Germany. *Source*: Google Earth. Loessnitztal river to the south; BR: production well; GWM: observation well; FWM: surface water level measurements

Materials and methods

The fate of the contaminants was evaluated through a twofold approach: (1) column experiments, consisting on laboratory work and inverse modeling; (2) solute transport modeling. The column tests were performed at the Geohydraulics laboratory at HTW Dresden, the chemical analyses were undertaken at the Institute of Water Chemistry at TU-Dresden, and the inverse modeling was done using the software CXTFIT 2.0 (Toride et al. 1995). The results were escalated to feed a contaminant transport model in MT3DMS (Zheng and Wang 1999), based on a groundwater flow model built using MODFLOW (McDonald and Harbaugh 1988). The selected site was Loessnitztal in East Germany where the water company ZWA Hainichen operates (Fig. 1).

Column experiments

Soil column experiments in the study of hydrogeological properties have been documented since the eighteenth century with the work of De la Hire in 1703, although their use in the chemistry and movement of solutes in pore-water started about two centuries later (Lewis and Sjöstrom 2010).

For this study, two stainless steel columns packed with sediments, each one with a diameter of 7.6 cm and a length of 50 cm, were run under saturated regime. The sediments came from the riverbed of the Loessnitztal River in East Germany, and the water was collected from the Elbe River at Dresden. The sediments were classified as poorly graded coarse sand, based on a sieve analysis using the standard DIN 18123 (DIN 2011), and the method described by the Unified Soil Classification System ASTM D2847 (ASTM 2006).

The whole experiment was set up in the Geohydraulics laboratory at HTW Dresden inside of a thermobox in order to control the temperature (Fig. 2). Two temperatures were used, 10 and 20 °C, because those are considered common water temperatures found in Colombian rivers (IDEAM 2010). A membrane pump made the water flow through the columns from top to bottom at a steady-state rate. Once the

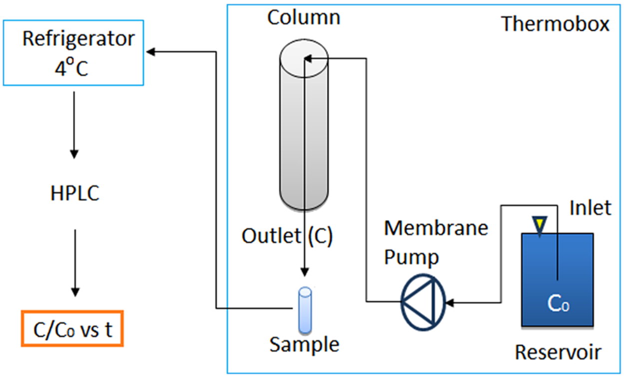

Fig. 2 Experimental setup for the column tests. C_0 is the initial concentration of each pesticide in the inlet reservoir; C is the final concentration of each pesticide in the outlet sample; HPLC: high-performance liquid chromatography

columns were saturated, a solution prepared at the Institute of Water Chemistry at TU-Dresden containing all five pesticides (ametryn, atrazine, carbofuran, diuron and propanil) dissolved in river water was introduced, and samples were taken at the outlet at different time intervals. These compounds were selected based on their availability and the possibility of being analyzed at the Institute.

In total, six experiments were run with a solution mix of approximately 10 mg of each pesticide in 1 L of filtered river water. Five hundred milliliters of such solution were mixed with 10 L of filtered river water (filter size = 1.2 µm). Before, and during, the column experiments, five tracer tests were performed using sodium chloride as conservative tracer to determine parameters such as porosity, pore volume (PV), residence time, Darcy's velocity and pore-water velocity. The first tracer test experiment was performed before the pesticides experiment started, mainly to check for any anomalies produced by problems in the packing or saturation, as recommended by Lewis and Sjöstrom (2010).

The outlet samples were preserved in a refrigerator at 4 °C before the high-performance liquid chromatography (HPLC) analysis at TU-Dresden. Also, a blank river water sample was analyzed to determine whether any of the pesticides under investigation were present; none was found. Inlet samples were also taken to determine the initial concentration, C_0, of each pesticide.

Finally, the breakthrough curves (BTCs) were plotted, and the most obvious outliers (caused by either human errors during the sampling process or instrumental errors during the analysis) were removed. An initial value of the retardation factor, R^*, was found for every component in each one of the experiments as the time (in PV) at which the relative concentration (C/C_0) was equal to 0.5. This value was used as the initial value for retardation factor, R, during the inverse modeling with CXTFIT.

Inverse modeling

The code CXTFIT 2.0, included in the freeware STANMOD v. 2.8. (Simunek et al. 1999), was used to determine the transport parameters associated with the column tests. STANMOD (STudio of ANalytical MODels) is a public domain computer software package that includes a modified and updated version of the CXTFIT code of Toride et al. (1995). The software estimates solute transport parameters from observed concentrations (inverse problem) using the advection dispersion equation (ADE) for one-dimensional transport of reactive solutes, subject to adsorption, fist-order degradation, and zero-order production in a homogeneous soil, as shown in Eq. (1) (Fetter 1999; Toride et al. 1995):

$$\frac{\partial}{\partial t}(\theta C + B_\mathrm{d} C^*) = \frac{\partial}{\partial x}\left(\theta D_\mathrm{L}\frac{\partial C}{\partial x} - v_x C\right) - \mu_\mathrm{l}\theta C - \mu_\mathrm{s} B_\mathrm{d} C^* + \xi_\mathrm{l}\theta + \xi_\mathrm{s} B_\mathrm{d} \tag{1}$$

where θ is the volumetric moisture content or porosity of the saturated media [L^3/L^3], C is the concentration of the solute in the water [M/L^3], B_d is the bulk density of the aquifer [M/L^3], C^* is the amount of solute sorbed per unit weight of solid [M/M], $\partial C/\partial t$ is the change in concentration with time [M/L^3/T], $\partial C/\partial x$ is the concentration gradient [M/L^3/L], v is the average linear velocity or pore-water velocity [L/T], D_L is the hydrodynamic dispersion coefficient (or just dispersion coefficient) parallel to the principal direction of flow (longitudinal) [L^2/T], μ_l and μ_s are the first-order decay coefficients for degradation of the solute in the liquid and sorbed phases, respectively, [1/T], and ξ_l [M/L^{3}T] and ξ_s [M/MT] are zero-order production terms for the liquid and sorbed phases, respectively.

Considering a linear sorption isotherm ($C^* = K_\mathrm{d} C$, where K_d is the distribution coefficient [M/L]), and assuming steady-state flow, Eq. (1) can be written as Eq. (2):

$$R\frac{\partial C}{\partial t} = D_\mathrm{L}\frac{\partial^2 C}{\partial x^2} - v_x\frac{\partial C}{\partial x} - \mu C + \xi \tag{2}$$

where R is the retardation factor, and μ and ξ are the combined first- and zero-order rate coefficients for the liquid and sorbed phases.

CXTFIT solves the inverse problem by minimizing an objective function, which consists of the sum of the squared differences between observed and fitted concentrations, using a nonlinear least-squares inversion approach based on the method of Levenberg–Marquardt (Marquardt 1963). The software also estimates the pore-water velocity (v), the dispersion coefficient (D), the retardation factor (R), the first-order degradation coefficient (μ), and/or the zero-order production coefficient (ξ), from observed concentration distributions versus time and/or distance.

In this particular case, a zero initial concentration, C_i, and a zero production coefficient, ξ, were chosen. Besides, a third-type inlet boundary condition (variable flux) was selected, because according to Toride et al. (1995) it is useful for most transport scenarios, assuming there is no dispersion outside the soil, and therefore mass is conserved.

In order to determine the transport and reaction parameters, CXTFIT requires the input of the pore-water velocity,v, and the initial values for D, R, and μ. The value of v was calculated during each column experiment, and the initial value of R is the one previously defined as R^* (from the column experiments). The initial values of D_L and μ were changed at the beginning of each run in order to obtain a better fit based on the minimum square error (MSE). In all cases, the software calculated fitted values for D, R and μ. Because dimensionless time and dimensional position were chosen as time and space units, all parameters calculated except D were dimensionless.

Contaminant transport modeling

The data from one of the column experiments were chosen to feed a contaminant transport model run in a transient state with the code MT3DMS (Zheng and Wang 1999), which was based on a steady-state groundwater flow model developed in Processing MODFLOW (PMWIN) version 5.3.3 (Chiang and Kinzelbach 1998). The procedure follows the same approach as for regular groundwater flow and solute transport; hence, we only present here the information relevant to our model. For specific procedures, the readers will be directed to original literature sources.

Groundwater flow model

The model was designed for the RBF site in Loessnitztal (East Germany), where the sediments for the columns were collected. The model included four production wells (BR), three observation wells (GWM), and four points for measurements of surface water level (FWM), as shown in Fig. 1. The area was discretized into 93 rows and 138 columns of 2×2 m, and one unconfined layer. The aquifer was considered to be homogeneous, with a hydraulic conductivity of 1.3×10^{-4} m/s (HTW Dresden 2012), and an effective porosity of 0.35 (value found with the column experiments).

The boundary conditions are shown in Fig. 3: constant head to the east and west, and RIVER to the south. The constant heads values came from the water level points FWM1 for the east boundary, and FWM4 for the west, all of them measured on the 27 April 2012. This date was selected because it lied within the time period selected to calculate the pumping rate for the production well BR3. For the RIVER boundary, the elevation of the river bottom was estimated with the river heads from the FWM points, a constant water level of 0.5 m, and a conductance of 4×10^{-4} m^2/s, calculated from an assumed thickness of the riverbed of 0.1 m and a permeability of the riverbed of 1×10^{-5} m/s (HTW Dresden 2012). The recharge over the main area was set to 3×10^{-9} m/s, and for the northern part of the model a recharge from runoff was set to 5×10^{-7} m/s, considering a precipitation of 200 mm/a, and a runoff area of approximately 275 m × 500 m.

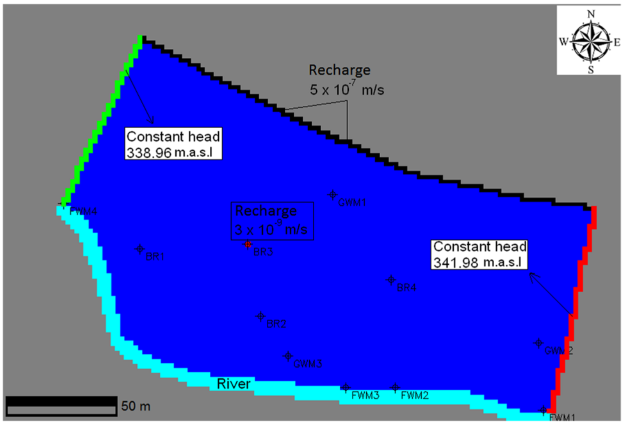

Fig. 3 Boundary conditions for the groundwater flow model

Two pumping scenarios from the discontinuously operated well BR3 were selected for calibration and validation. Scenario 1 was used for calibration with a pumping rate of 9.5×10^{-4} m^3/s, assuming a 24 h/day pumping, whereas scenario 2 was used for validation with an extraction rate of 3.95×10^{-4} m^3/s, considering only 10 h/day pumping. The time period from 26 April at 8:15 am to 29 May at 8:30 am was selected in order to calculate the total abstraction from well BR3. During that time the well pumped a total volume of 2322 m^3 in 680 h, approximately. The particle tracking software PMPATH (Chiang and Kinzelbach 1994) was used to determine the flowpath-lines both for water free of pesticides and for each of the pesticides.

Contaminant transport model

MT3DMS is a modular 3-D multi-species transport model for simulation of advection, dispersion, and chemical reactions of contaminants in groundwater systems (Zheng and Wang 1999). The model is based on the partial differential equation describing the fate and transport of contaminants of species k in three-dimensional, transient groundwater flow systems, as shown in Eq. (3):

$$\frac{\partial(\theta C_k)}{\partial t} = \frac{\partial}{\partial x_i}\left(\theta D_{ij}\frac{\partial C_k}{\partial x_j}\right) - \frac{\partial}{\partial x_i}\left(\theta v_i C_k\right) + q_s C_{k,s} + \sum R_n \tag{3}$$

where C_k is the dissolved concentration of species k [ML^{-3}], θ is the porosity of the subsurface medium [dimensionless], t is time [T], x_i is the distance along the respective coordinate axis [L], D_{ij} is the hydrodynamic dispersion coefficient tensor [L^{2}T^{-1}], v_i is the seepage or linear pore-water velocity [LT^{-1}] ($v_i = q_i/\theta$), q_s is the volumetric flow rate per unit volume of aquifer representing fluid sources (positive) and sinks (negative) [T^{-1}], $C_{k,s}$ is the concentration of the source or sink flux for species k [ML^{-3}], and $\sum R_n$ is the chemical reaction term [ML^{-3}T^{-1}] (general biochemical and geochemical reactions, i.e., aqueous-solid surface reaction (sorption) and first-order rate reaction).

Before choosing one of the scheme solutions for the advection term that MT3DMS offers, the Peclet number, Pe, was estimated using Eq. (4) in order to determine whether or not the problem was advection-dominated (Chiang 2005).

$$Pe = \frac{|v|L}{D} \tag{4}$$

where $|v|$ is the magnitude of the seepage velocity vector $[\mathrm{LT}^{-1}]$, L is a characteristic length commonly taken as the grid cell width [L], and D is the dispersion coefficient $[\mathrm{L}^2\mathrm{T}^{-1}]$.

For this particular case, Pe was calculated in two ways: Pe_1 using v from experiment E 3-1 (the experiments whose results were used in the contaminant transport model) and L as the length of the column, and Pe_2 calculating v from the groundwater flow model and L as the width of the grid cell. In both cases, the value for D was the average of the dispersion coefficients of the pesticides.

Based on the calculated Peclet numbers ($Pe_1 = 4.5$ and $Pe_2 = 17$), the problem is not advection-dominated, and therefore numerical dispersion during the solution of the transport equation is not expected to be a significant problem (Zheng and Wang 1999). For this kind of problem, the same authors suggest that the standard finite difference method can be used for greater computation efficiency and to obtain first approximations in the initial stages of modeling. Therefore, the Upstream Finite Difference solution scheme was selected for this study.

In order to calculate the value of the longitudinal dispersion coefficient, D_L, Eqs. (5) and (6) were used, with the values of pore-water velocity, v_i, and dispersion coefficient, D, found with CXTFIT.

$$D_\mathrm{L} = \alpha_\mathrm{L} v_\mathrm{i} + D^* \rightarrow \alpha_\mathrm{L} = \frac{D_\mathrm{L} - D^*}{v_\mathrm{i}} \tag{5}$$

$$D^* = \omega D_\mathrm{d} \tag{6}$$

where D_L is the hydrodynamic dispersion coefficient parallel to the principal direction of flow (longitudinal) $[\mathrm{L}^2\mathrm{T}^{-1}]$ (D found through CXTFIT), α_L is the longitudinal dynamic dispersivity [L], v_i is the average linear velocity in the principal direction of flow $[\mathrm{LT}^{-1}]$ (v from column experiment E 3-1), D^* is the effective diffusion coefficient $[\mathrm{L}^2\mathrm{T}^{-1}]$, D_d is the molecular diffusion coefficient $[\mathrm{L}^2\mathrm{T}^{-1}]$, and ω is a coefficient related to tortuosity [dimensionless], which measures the effect of the shape of the flowpath of a water molecule in a porous media. For laboratory experiments the values of ω range between 0.01 and 0.7, according to Perkins and Johnson (1963) and Freeze and Cherry (1979), respectively. In order to evaluate the sensibility of the results to D^* three values of α_L were calculated: α_1 with ω equal to 0.7, α_2 with ω equal to 0.01, and α_3 with ω equal to zero (when the effective diffusion coefficient is not taken into account).

Fried (1975) defined the scale effect of dispersion as the influence of the flow length on the value of α_L, explaining that the greater the flow length, the larger the value of longitudinal dispersivity needed to fit the data to the ADE. Afterward, different authors came up with empirical equations based on measurements of dispersivity in the field, as shown in Eqs. (7)–(12).

$$\alpha_\mathrm{L} = 0.1L \quad \text{(Lallemand-Barres and Peaudecerf 1978)} \tag{7}$$

$$\alpha_\mathrm{L} = 0.83(\log\ L)^{2.414} \quad \text{(Xu and Eckstein 1995)} \tag{8}$$

$$\alpha_\mathrm{L} = 0.0175L^{1.46} \quad \text{for} \quad L \le 3500\ \mathrm{m} \quad \text{(Neuman 1990)} \tag{9}$$

$$\alpha_\mathrm{L} = 0.0169L^{1.53} \quad \text{for} \quad (L \le 100\ \mathrm{m}) \quad \text{(Neuman 1990)} \tag{10}$$

$$\alpha_\mathrm{L} = 0.017L^{1.5} \quad \text{for} \quad (L \le 3460\ \mathrm{m}) \quad \text{(Neuman 1990)} \tag{11}$$

$$\alpha_\mathrm{L} = 0.32L^{0.83} \quad \text{for} \quad L > 100\ \mathrm{m} \quad \text{(Neuman 1990)} \tag{12}$$

In terms of the chemical reactions, a linear equilibrium sorption isotherm was chosen, as well as the possibility to simulate radioactive decay or biodegradation. The parameters that MT3DMS require for these two options are bulk density of the porous medium, ρ_b $[\mathrm{ML}^{-3}]$, distribution coefficient, K_d $[\mathrm{L}^3\mathrm{M}^{-1}]$, 1st-order reaction rate for the dissolved phase $[\mathrm{T}^{-1}]$, and 1st-order reaction rate for the sorbed phase $[\mathrm{T}^{-1}]$.

The bulk density was calculated from Eq. (13):

$$n = 100\left[1 - \frac{\rho_\mathrm{b}}{\rho_\mathrm{d}}\right] \tag{13}$$

where n is the porosity of the porous medium [%], and ρ_d is the particle density $[\mathrm{ML}^{-3}]$. For most rocks and soils, the particle density is about 2.65 $\mathrm{g/cm}^3$, which is the density of quartz (Fetter 1999).

The distribution coefficient, K_d, was found using Eq. (14):

$$R = 1 + \frac{\rho_\mathrm{b} K_\mathrm{d}}{\theta} \tag{14}$$

where R is the retardation factor found with the inverse modeling, and θ is the porosity of the aquifer found with the column experiments.

Because it was not possible to determine individual degradation parameters for the reaction rates of the liquid and sorbed phases, it was decided to assign the value of the degradation coefficient μ obtained with CXTFIT to the 1st-order reaction rate for the dissolved portion, and a value of 0 for the 1st-order reaction rate for the sorbed phase, which is a simplification appropriate for some pesticide–soil combinations according to Toride et al. (1995).

The parameter μ found through inverse modeling is, in fact, a combination of the first-order degradation coefficient in the liquid and in the adsorbed phases, i.e., μ_l and μ_s, respectively (Toride et al. 1995), as shown in Eq. (15):

$$\mu = \mu_l + \frac{\rho_b K_d \mu_s}{\theta}. \tag{15}$$

Because only degradation in the liquid phase was considered, the equation is reduced to $\mu = \mu_l$. As explained before, μ is a dimensionless value that has to be converted into a dimensional one in order to use it in MT3DMS. This can be done by applying Eq. (16), as follows (Toride et al. 1995):

$$\mu = \frac{\mu^E v}{L} \tag{16}$$

where μ is the value of the degradation [T^{-1}], μ^E is the value found through inverse modeling [dimensionless], v is the seepage velocity from the column experiment [LT^{-1}], and L is the length of the column [L] (equal to 50 cm).

The simulation time for the contaminant transport model was divided into three periods, each one of different duration (Table 1). For this specific exercise, a contaminant river source was chosen, and it was assumed an accidental spill on the river with a concentration of 30 g of contaminant per liter of water. Such concentration was applied during the second period of the simulation time.

In order to test the sensitivity of the model to longitudinal and transverse dispersivity (α_L and α_T, respectively) and to degradation, four (4) different scenarios were considered during the contaminant transport simulation (Table 2): in scenarios 1 and 4, both, α_L and α_T (through the ratio α_L/α_T) were kept constant, but only in scenario 1 degradation was also considered for the contaminant transport; in scenarios 2 and 3, degradation was also considered, but either α_L or α_T was changed after each run of the model.

Table 1 Time periods defined for the transient simulation

Period	Length (s)	Length (days)	Time steps
1	3.2×10^7	369.2	1
2	10^5	1.16	1
3	6.3×10^7	729.2	1

Table 2 Scenarios considered during contaminant transport modeling

Scenario	α_L (m)[a]	α_T/α_α[b]	Degradation
1	Constant	Constant	Yes
2	Varying	Constant	Yes
3	Constant	Varying	Yes
4	Constant	Constant	No

[a] Longitudinal dispersion coefficient (α_L)

[b] Transverse dispersion coefficient (α_T)

Results

Column experiments

Table 3 shows the parameters obtained from the tracer tests. The porosity of column 1 shows almost no variation during all the experiments, independently of the temperature (0.34 at 20 °C, and 0.35 at 10 °C), but for column 2 the change is more significant (0.32 at 10 °C and 0.36 at 20 °C). Considering the way porosity was calculated, this increment can be attributed to the increase in t_{50} in TT 5-2 in comparison with TT 2-2, which could be caused by the rearrangement of the sediments during the time of the experiments, as a consequence of problems with the uniformly packing of the columns. It is possible that a similar process took place in column 1 but in a lesser degree.

A breakthrough curve (BTC) was obtained for each column experiment, but here only the one for experiment E 3-1 is shown (Fig. 4), because the results of this particular experiment were the ones chosen to feed the contaminant transport model. Each contaminant column experiment lasted about 198 h (for a total of 1190 h) and an average of 22 outlet samples and 7 inlet samples were analyzed. In all the cases, the concentration in the outlet never reached the same value as the concentration in the inlet ($C_0 > C$) due to degradation and sorption processes. The maximum average removal was achieved for diuron (70%), followed by carbofuran (77%), ametryn (84%), and atrazine (97%).

The pesticide that showed the lowest C/C_0 ratio was propanil, which was almost completely missing in the outlet samples, with a maximum concentration barely reaching 14% of the initial (Fig. 5). The samples were additionally tested for 3,4-dichloroaniline (being the main degradation product of propanil according to the Hazardous Substances Data Bank (HSDB), a database of the National Library of Medicine's TOXNET system; http://toxnet.nlm.nih.gov), and it was found that the concentration of this compound increased with time (Fig. 6).

3,4-Dichloroaniline is not only the main degradation product of the herbicide propanil, but also one of the metabolites of diuron, and in both cases it is also a more toxic substance than its two parental compounds (http://toxnet.nlm.nih.gov). Considering that the time required for the chemical concentration of propanil to decline to 50% of the amount of application in a water–sediment system is 4.4 days, whereas that of diuron is 75.5 days, it can be inferred that most of the dichloroaniline found in the inlet water came from the degradation of propanil.

This and more information on the pesticides used in this study can be found in the Pesticides Properties Data Base (PPDB), which is a comprehensive relational database of pesticide physicochemical and ecotoxicological data

Table 3 Parameters obtained from the tracer tests (TT)

Parameter	TT 1-1	TT 2-2	TT 3-1	TT 4-1	TT 5-2
T (°C)	20	10	10	20	20
Associated pesticide experiment[a]	N/A	E 2-2	E 3-1	E 4-1	E 4-2
Duration time (min)	2585	12,635	11,755	8120	8120
Q (ml/min)	0.98	0.56	0.58	0.46	0.55
t_{50} (min)[b]	793	1307.5	1372.5	1668	1498
Pore-water velocity (cm/min)[c]	0.063	0.038	0.036	0.03	0.033
Darcy's velocity (cm/min)[d]	0.022	0.012	0.013	0.010	0.012
Porosity[e]	0.34	0.32	0.35	0.34	0.36
Pore volume (cm^3)[f]	781	727	797	760	822

The name of the tracer test is given by the letters TT (Tracer Test) followed by the sequence number of the experiment (1–5), and ending in the column number (1 or 2). Thus, TT 3-1 was the third tracer test performed, and it was run in column number 1

[a] For the pesticides experiments, the nomenclature is similar to that of tracer tests, with TT changed by E. The first tracer test was run without any pesticides

[b] Time at which C/C_0 was equal to 0.5, i.e., when half of the solute had left the column

[c] The length of the column divided by t_{50}

[d] The average discharge (Q) divided by the cross-sectional area of the column

[e] Derives from the division of Darcy's velocity by the pore-water velocity

[f] Volume of the column times the porosity

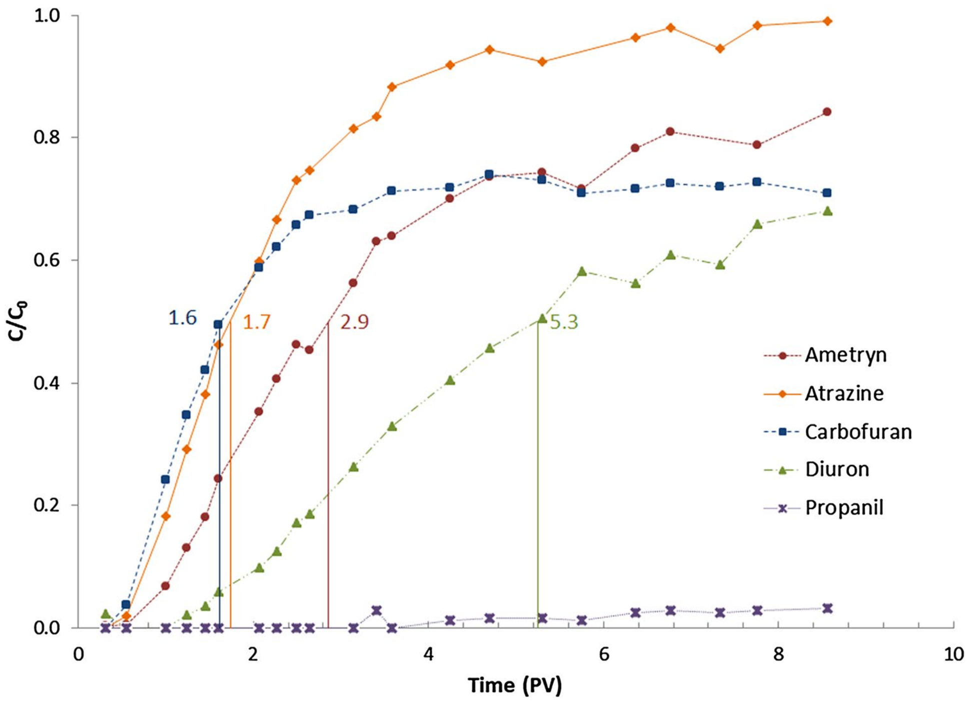

Fig. 4 Results of column experiment E 3-1: column 1 at 10 °C. The numbers next to the line graphs correspond to the values of retardation factor (R^*) for each pesticide; time is expressed in pore volume (PV)

developed by the Agriculture and Environment Research Unit (AERU) at the University of Hertfordshire (England), and can be accessed online at http://sitem.herts.ac.uk/aeru/ppdb/en/index.htm.

Inverse modeling

The results of the inverse modeling are shown in Table 4. Carbofuran was not modeled for experiment E 4-1 and E

Fig. 5 Concentration of propanil in the outlet samples for the six column experiments. Time is expressed in pore volume (PV)

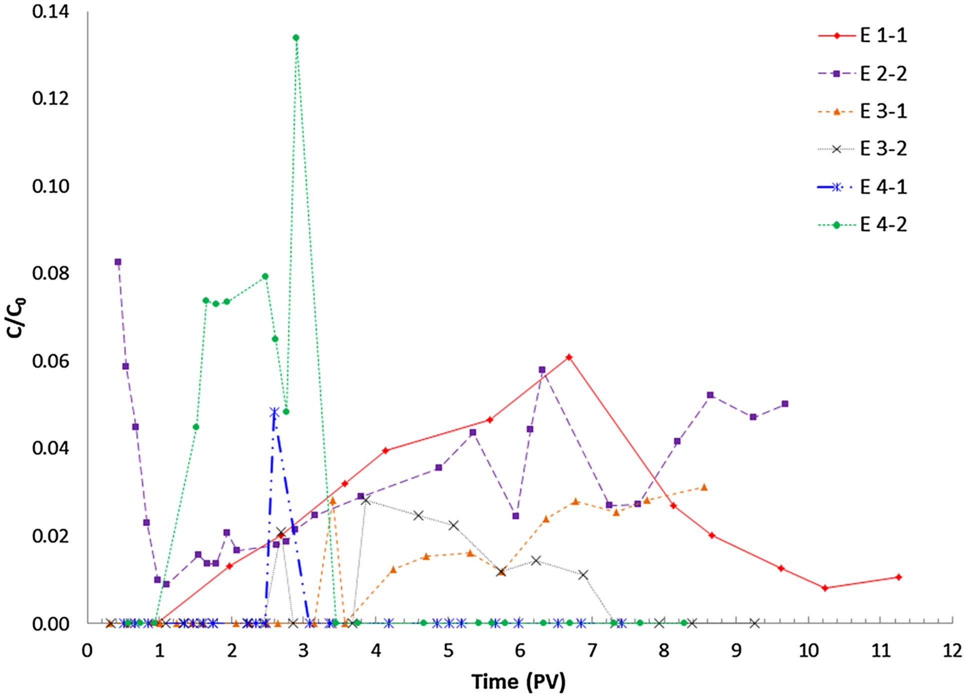

Fig. 6 Concentration of 3,4-dichloroaniline in the outlet samples for the six column experiments. The *y*-axis shows the concentration as the area under the curve, and the *x*-axis shows the time in minutes

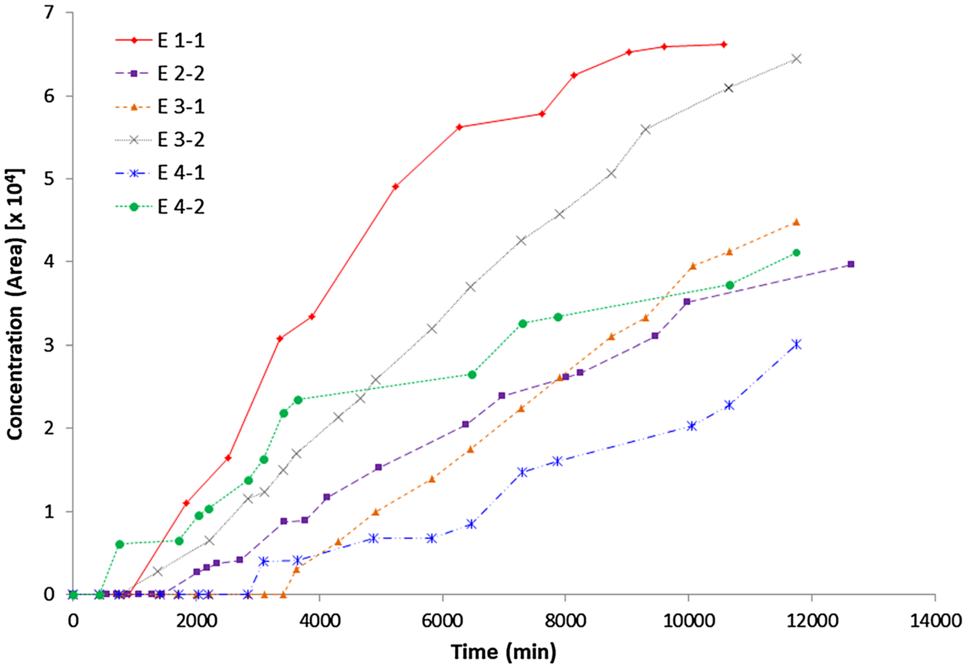

4-2 because the results of the column tests presented some inconsistencies due to problems being experimented at the laboratory at TU-Dresden.

The results from Table 4 indicate that, in average, carbofuran shows the lowest retardation factor ($R = 1.2$), but the highest degradation coefficient ($\mu = 0.24$); diuron has the highest retardation factor ($R = 3.9$) and dispersion coefficient ($D = 1.6$); atrazine presented the lowest dispersion coefficient ($D = 0.6$), and a degradation coefficient so low ($\mu = 0.02$) that the substance can be considered non-degradable. In general, the results of retardation factor for atrazine are similar to those reported in alluvial aquifers by Agertved et al. (1993)

Table 4 Results of the inverse modeling with CXTFIT for each pesticide and each experiment

Pesticide	Experiment	Observed		Fitted			MSE $(10^{-3})^{*}$	R^{2**}
		v^{a} (cm/min)	R^{*b}	D^{c} (cm^2/min)	R^{d}	μ^{e}		
Ametryn	E 1-1	0.054	2.5	0.48	2.0	2.1E−01	3.358	0.9600
	E 2-2	0.038	2.5	1.27	2.1	4.8E−02	0.872	0.9905
	E 3-1	0.037	2.9	0.44	2.4	1.6E−01	0.230	0.9975
	E 3-2	0.039	2.4	1.04	2.0	1.6E−01	0.375	0.9945
	E 4-1	0.030	3.1	0.44	2.6	1.6E−01	0.328	0.9964
	E 4-2	0.034	2.6	2.66	1.9	5.0E−05	0.689	0.9884
Atrazine	E 1-1	0.054	1.7	0.62	1.5	4.9E−02	0.518	0.9943
	E 2-2	0.038	1.6	0.91	1.4	9.0E−09	0.496	0.9954
	E 3-1	0.037	1.7	0.41	1.7	2.3E−02	0.281	0.9976
	E 3-2	0.039	1.5	1.35	1.3	9.0E−09	0.789	0.9909
	E 4-1	0.030	1.8	0.04	1.7	6.5E−02	0.302	0.9972
	E 4-2	0.034	1.7	0.18	1.3	2.6E−04	0.409	0.9936
Carbofuran	E 1-1	0.054	1.5	0.25	1.1	3.0E−01	3.161	0.9171
	E 2-2	0.038	1.5	1.00	1.3	1.6E−01	0.344	0.9942
	E 3-1	0.037	1.6	0.34	1.4	2.9E−01	0.163	0.9972
	E 3-2	0.039	1.6	1.57	1.1	2.2E−01	0.265	0.9930
Diuron	E 1-1	0.054	4.1	0.69	3.3	2.4E−01	0.358	0.9961
	E 2-2	0.038	4.7	1.39	4.0	0	0.253	0.9968
	E 3-1	0.037	5.3	0.44	4.2	2.7E−01	0.250	0.9963
	E 3-2	0.039	4.2	1.46	3.4	1.1E−01	0.368	0.9939
	E 4-1	0.030	5.5	1.00	5.6	8.6E−08	0.456	0.9896
	E 4-2	0.034	5.4	4.65	2.9	1.9E−07	1.193	0.9685

[a] Pore-water velocity from column experiments

[b] Retardation factor from column experiments [dimensionless]

[c] Dispersion coefficient

[d] Retardation factor from inverse modeling with CXTFIT [dimensionless]

[e] Degradation coefficient [dimensionless]

[*] Minimum square error

[**] Correlation coefficient

(R = 1.2), by Pang and Close (1999) (R = 1), and for column experiments by Mao and Ren (2005) ($1.82 \leq R \leq 1.95$).

Even though sorption and degradation processes are affected by temperature (Paraiba and Spadotto 2002), in this particular study it was not possible to find any clear trend relating the two different temperatures (10 °C and 20 °C) with the coefficients of dispersion and degradation, D and μ, or with the retardation factor, R. Furthermore, degradation is not easily interpreted from the BTCs and its values are not consistent from experiment to experiment, making it the parameter that shows a more unpredictable behavior of the three calculated with CXTFIT.

The best fitted BTC obtained from the inverse modeling (solid line), and the observed values from the column experiments (only markers) for experiment E 3-1 are depicted in Fig. 7. This graph also includes the BTC for the tracer test TT 3-1, whose value of effective porosity was used to calculate the time in pore volumes at which each sample was taken. Because the tracer used is a conservative contaminant, NaCl, the relative concentration, C/C_0, at 1 PV is equal to 0.5 (center of mass), i.e., $R = 1$ and $\mu = 0$.

The shapes of the BTCs are directly related to the dispersion coefficient and degradation factor (Fetter 1999).

Fig. 7 Results from the inverse modeling (fitted) and column experiment (obs) E 3-1 for all pesticides, except propanil. The observed values are shown with markers and the fitted values with lines; time is given in pore volume (PV); the breakthrough curve of tracer test TT 3-1 is also shown as a discontinued line

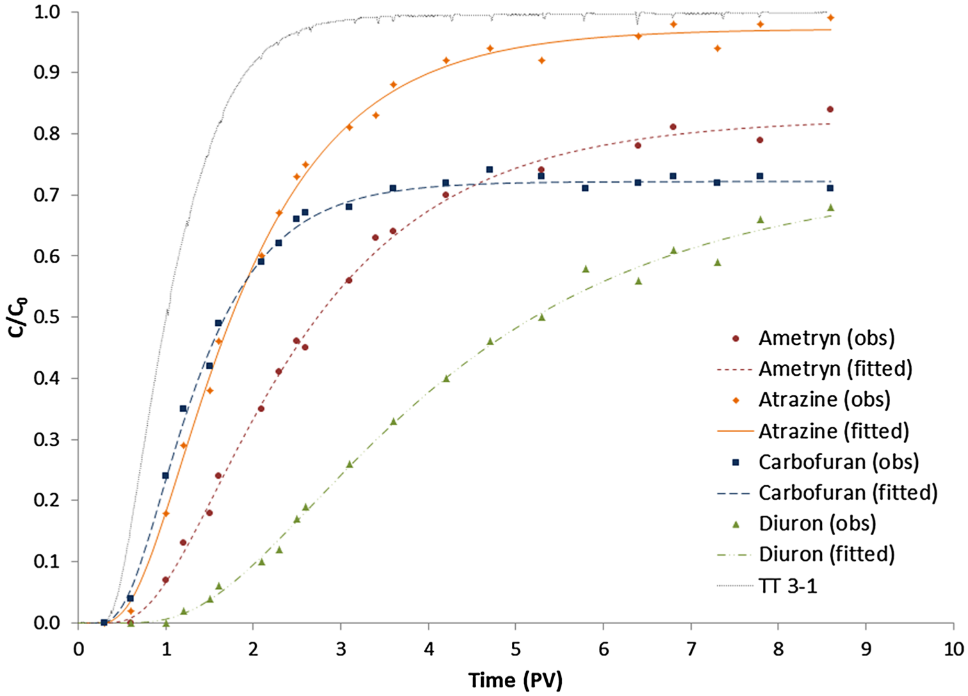

Thus, the skewness of the curves reflects the degree of dispersion, i.e., the higher the dispersion coefficient, the higher the skewness of the BTC. Also, the higher the degradation, the lower is the total amount of contaminant that appears at the bottom of the column, which means that the relative concentration, C/C_0, will be further away from the unit. Since the retardation factor is a measure of adsorption behavior, or how tightly the pesticide binds or sticks to soil particles (Eckhard 1999), the higher the value of R the stronger the substance fixes onto soil material and the slower it appears at the bottom of the column.

From the BTCs is clear that, in all cases, diuron presents the highest skewness, which coincides with the higher values of dispersion coefficient for this pesticide in most of the experiments. In terms of degradation, the BTCs show that atrazine is always the component whose final relative concentration is closest to 1, indicating that the degradation of such compound is the lowest of all the studied pesticides.

The values of μ presented in Table 4 show that degradation is not always lowest for this particular pesticide, but vary from experiment to experiment between atrazine and diuron. These could be because these two pesticides are less (or not at all) degraded under aerobic conditions than they would be under anoxic conditions (Jekel and Grischek 2003). One of the reasons why the low degradation of diuron cannot be inferred from the BTCs could be the fact that the duration time of the experiments was not long enough for the pesticide to leave the column due to its high retardation factor, which translates into a slower travel velocity than the rest of the studied compounds.

Contaminant transport modeling

Groundwater flow model

As explained in "Groundwater flow model" section, the groundwater flow model considered two different pumping scenarios: scenario 1 (9.5×10^{-4} m^3/s) for calibration and scenario 2 for validation (3.95×10^{-4} m^3/s). The resulting piezometric heads for calibration presented a normalized root-mean-square error (NRMSE) of 0.026%, and a correlation with the observed heads of 0.993; for validation, the NRMSE was 0.031% and the correlation was 0.996. The parameters used for calibration were the hydraulic conductivity and the thickness of the aquifer, being the latter a more sensitive parameter than the former.

Using backward particle tracking, the capture zone of well BR3 and the flowlines were extracted (Fig. 8). For illustration purposes, the step length was set to 60 days and the retardation factor was changed for each pesticide, according to Table 5. The retardation factor,R, for river water without pesticides is assumed to be 1.

The results of travel times (earliest arrival) in days and the values of R from inverse modeling of experiment E 3-1 for each pesticide and for river water are presented in Table 5.

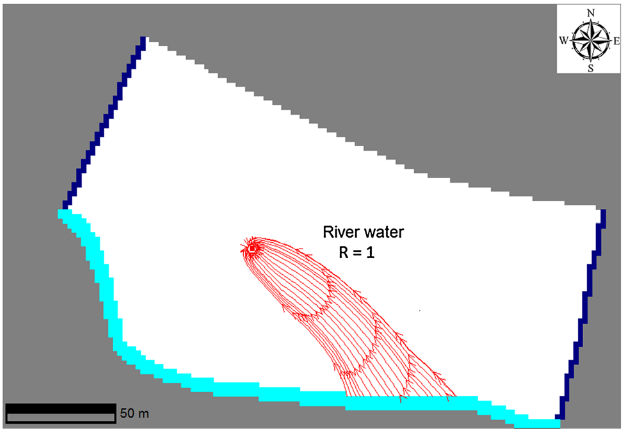

Fig. 8 Flowlines and travel time marks (every 60 days) for river water ($R = 1$)

Table 5 Retardation factor and average travel time from the river to the well for each pesticide and for river water

Pesticide	R^a	Average travel time (days)
River water	1.0	150
Ametryn	2.4	300
Atrazine	1.7	210
Carbofuran	1.4	180
Diuron	4.2	540

[a] Retardation factor found through inverse modeling for column experiment E 3-1

As expected, the higher the retardation factor, the longer the travel time from the river to the well. These results only take into account transport by advection and completely disregard the effect of dispersion and degradation of the contaminant.

Contaminant transport model

The results from column experiment E 3-1 showed the lowest MSE for all the pesticides (see Table 4) and, therefore, were selected to feed the contaminant transport model. The results for longitudinal dispersivity, α_L, calculated with Eq. (5), using an effective diffusion coefficient, D^*, calculated with Eq. (6), are shown in Table 6. Despite that three different values for the tortuosity coefficient, ω, were used to estimate D^* (0, 0.01 and 0.7), they represented only a maximum difference of 7×10^{-3} cm in the value of the longitudinal dispersivity, proving that Eq. (5) is not very sensitive to the effective diffusion coefficient.

In order to test the scale effect of dispersion, and considering that the length of the flowpath between the river and BR3 is approximately 95 m (result from flow modeling, see Fig. 8), the value of α_L was calculated using the empirical equations with no limits for flowpaths or for flowpaths shorter than 100 m, i.e., Eqs. (7)–(11). The results in Table 7 show variations of one order of magnitude between the lowest and the highest values of α_L (9.5 m and 17.9 m, respectively), with an average of 12.2 m, in contrast to the results of Table 6 that show almost no variation.

In this way, the scale effect of dispersion due to flow length described by Fried (1975) becomes clearer and supports the importance of testing the sensitivity of the solute transport model to different values of both, longitudinal and transverse dispersivity; hence, the four scenarios selected for simulation (Table 8).

Scenario 1 was selected to estimate the average behavior of the contaminant plumes (and concentrations reaching the pumping well), setting α_L equal to 12.2 m (the average from Table 7), and α_T as 10% of α_L, which is the value suggested by Fetter (1999) when no information on the parameter is available. In scenario 2, the effect of the longitudinal dispersivity was evaluated, by leaving constant the ratio α_T/α_L ($\alpha_T = 0.1\alpha_L$), but using for α_L all the values found with the empirical equations (Table 7), i.e., 4.3, 9.5, 13.5, 15.7, and 17.9 m. The effect of the transverse dispersivity was tested in scenario 3, where the average value of α_L was used, while varying the ratio α_T/α_L like this: 1, 0.5, 0.1, 0.01 and 0.001. In scenario 4, the conditions were similar to scenario 1, but degradation was not considered in the simulation, in order to test the sensibility of the model to such parameter. Finally, the horizontal and the vertical transverse dispersivity were assumed to be the constant during the simulations, because the porous medium was assumed to be homogeneous and isotropic.

Scenario 1 The contaminant plumes and the breakthrough curves for each pesticide at the end of the 3-year simulation period are shown in Fig. 9. The center of mass of atrazine (Fig. 9b) has almost completely left the domain, whereas those of carbofuran (Fig. 9c) and diuron (Fig. 9d) have not even reached the well. Also, even though the ratio α_T/α_L was the same for all contaminants, carbofuran presents the smallest dispersion in the direction perpendicular to the flow, whereas atrazine displays the highest of all the studied pesticides, which can be observed in both the contaminant plumes and the BTCs (the thinner the BTC, the narrower the contaminant plume in the direction perpendicular to the flow). If only the retardation factor was considered, as in Table 5, carbofuran should be the pesticide traveling faster, because it had the lowest R during column experiment E 3-1. However, the results of the contaminant transport model demonstrate the importance of dispersion in the fate of contaminants in the subsoil, as carbofuran presented the lowest dispersion (0.34), thus remaining in the aquifer for a longer time than atrazine and even ametryn. Diuron, being the pesticide with the

Table 6 Values of longitudinal dispersivity found from the equation for hydrodynamic dispersion coefficient

Pesticide	D_L[a] (cm^2/min)	D_d[b] (cm^2/min)	D_1^*[c] (cm^2/min)	D_2^*[d] (cm^2/min)	α_1[e,f] (cm)	α_2[g] (cm)	α_3[h] (cm)
Ametryn	0.44	3.4E−04	2.4E−04	3.4E−06	11.885	11.892	11.892
Atrazine	0.41	3.4E−04	2.4E−04	3.4E−06	11.075	11.081	11.081
Carbofuran	0.34	3.2E−04	2.3E−04	3.2E−06	9.183	9.189	9.189
Diuron	0.44	3.2E−04	2.2E−04	3.2E−06	11.886	11.892	11.892

[a] Longitudinal dispersion coefficient = dispersion coefficient found through inverse modeling with CXTFIT for column experiment E 3-1

[b] Molecular diffusion coefficient (specific for each pesticide)

[c] Effective diffusion coefficient calculated with $\omega = 0.7$, where ω is a dimensionless coefficient related to tortuosity

[d] Effective diffusion coefficient calculated with $\omega = 0.01$

[e] Longitudinal dynamic dispersivity calculated with D_1^*

[f] The value for pore-water velocity (v) used to calculate the longitudinal dispersivity was 0.037 cm/min, and corresponds to the velocity found during inverse modeling with CXTFIT for column experiment E 3-1

[g] Longitudinal dynamic dispersivity calculated with D_2^*

[h] Longitudinal dynamic dispersivity calculated with $D^* = 0$

Table 7 Longitudinal dispersivity calculated with different empirical equations for $L = 95$ m

Authors	Equation[a]	α_{L} (m)[b]
Lallemand-Barres and Peaudecerf (1978)	$\alpha_{\mathrm{L}} = 0.1L$	9.5
Xu and Eckstein (1995)	$\alpha_{\mathrm{L}} = 0.83(\log L)^{2.414}$	4.3
Neuman (1990) ($L \leq 3500$ m)	$\alpha_{\mathrm{L}} = 0.0175L^{1.46}$	13.5
Neuman (1990) ($L \leq 100$ m)	$\alpha_{\mathrm{L}} = 0.0169L^{1.53}$	17.9
Neuman (1990) ($L \leq 3460$ m)	$\alpha_{\mathrm{L}} = 0.017L^{1.5}$	15.7
	Average	12.2

[a] L represents the length of the flowpath between the river and the pumping well BR3

[b] Longitudinal dispersivity

Table 8 Details on the four scenarios considered for the simulations

Scenario	α_{L} (m)[a]	$\alpha_{\mathrm{T}}/\alpha_{\alpha}$[b]	Degradation
1	12.2	0.1	Yes
2	Varying	0.1	Yes
3	12.2	Varying	Yes
4	12.2	0.1	No

[a] Longitudinal dispersion coefficient (α_{L})

[b] Transverse dispersion coefficient (α_{T})

highest retardation factor (4.2), was expected to be the slowest.

When looking at the maximum concentrations in the BTCs, the effect of the degradation coefficient, μ, is made clearer. Thus, atrazine, which was the pesticide with the lowest value of μ (0.023) during the inverse modeling, is the one with the highest concentration at the center of the plume, whereas carbofuran and diuron, with the highest degradation coefficients (0.288 and 0.267, respectively), are the components with the lowest concentrations.

Table 9 shows, for each pesticide, the maximum concentration reaching the well ($C_{\max}$), and the correspondent removal when compared to the initial concentration in the river water due to the assumed accidental spill (30 g/L). Even for atrazine, which is the pesticide showing the least removal, hence posing the highest risk of water supply, the maximum concentration in the well would be only 0.013% of the input concentration. The differences in the percentage removal achieved with column experiments (a maximum of 30%) and with the numerical modeling emphasize the importance of the length of the flowpath, i.e., scale effect of the dispersion coefficient.

Scenario 2 The differences in BTCs, when changing the values of longitudinal dispersivity, α_{L}, become more evident when having all the BTCs for each pesticide in the same graph (Fig. 10 above). In all cases, the arrival time of the maximum concentration at well BR3 increases with a decrease in the value of the longitudinal dispersivity, with this inverse relationship being clearer for atrazine (Fig. 10c).

In general, an exponential behavior between the maximum concentration detected at the well and the time at which it was detected can be observed in Fig. 10: Toward the lower values of α_{L}, there will be a threshold where the maximum concentration asymptotically reaches a minimum

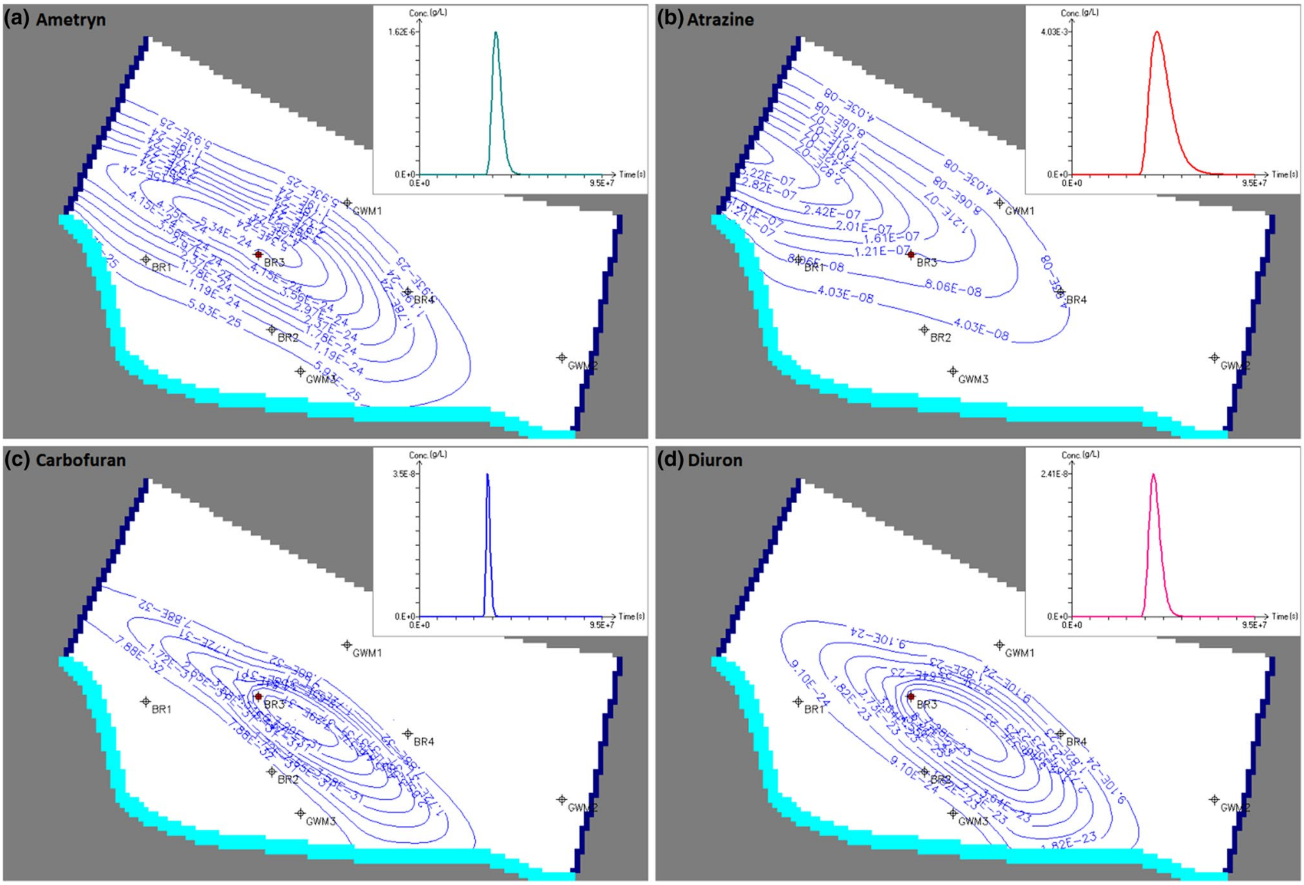

Fig. 9 Contaminant plume and breakthrough curve for the contaminants in scenario 1: $\alpha_L = 12.2$ m; $\alpha_T = 0.1\alpha_L$

Table 9 Results of simulation scenario 1

Pesticide	C_{arrival}[a] (mg/L)	$C_{\max}$[b] (mg/L)	% Removal[c]	Log removal[d]
Ametryn	1.5×10^{-18}	1.6×10^{-3}	99.99999460	7.3
Atrazine	7.0×10^{-13}	4.0	99.98656667	3.9
Carbofuran	6.6×10^{-13}	3.5×10^{-5}	99.99999988	8.9
Diuron	2.9×10^{-18}	2.4×10^{-5}	99.99999992	9.1

[a] First concentration detected at borehole BR3

[b] Maximum concentration detected at borehole BR3

[c] Comparing initial concentration of each pesticide in the river water (30 g/L) with the maximum concentration reaching the well

[d] Removal (%) = $100 - 10^{(2-x)}$, where x is the log removal

value, whereas the time from spilling associated with such concentration will continue to increase. On the other side of the spectrum, i.e., for high values of α_L, the maximum value of concentration will keep on increasing but the time will remain somehow constant. This behavior is especially noticeable for ametryn (Fig. 10b), carbofuran (Fig. 10e) and diuron (Fig. 10g), but not as much for atrazine (Fig. 10d), which is the pesticide that presented the maximum concentration in the center of the plume and more sensitivity to the changes of longitudinal dispersivity in terms of the shape of the BTC. Thus, longitudinal dispersivity represents not only lower concentrations at the pumping well, but also longer detection time of the contaminant in the well.

Scenario 3 Figure 11 shows the BTCs for the four pesticides at different ratios of transverse and longitudinal dispersivity. The behavior is similar for either value of α_L when it comes to the maximum concentration measured at the pumping well BR3, i.e., the concentration increases with lower values of α_T/α_L until certain threshold is reached where the increment in concentration is insignificant. This behavior is valid for all pesticides for the ratio values of 0.01 and 0.001, so it could be assumed that it will happen even for lower ratios. The difference in concentrations between the two graphs of the same pesticide is related to the values of longitudinal dispersivity.

The effects of the different ratios α_T/α_L on the contaminant plume of ametryn are shown in Fig. 12 (only graphs for extreme values of the ratio transverse/longitudinal dispersivities are presented, i.e., 0.001 and 1). The results for ametryn were selected as an example of what appears to be

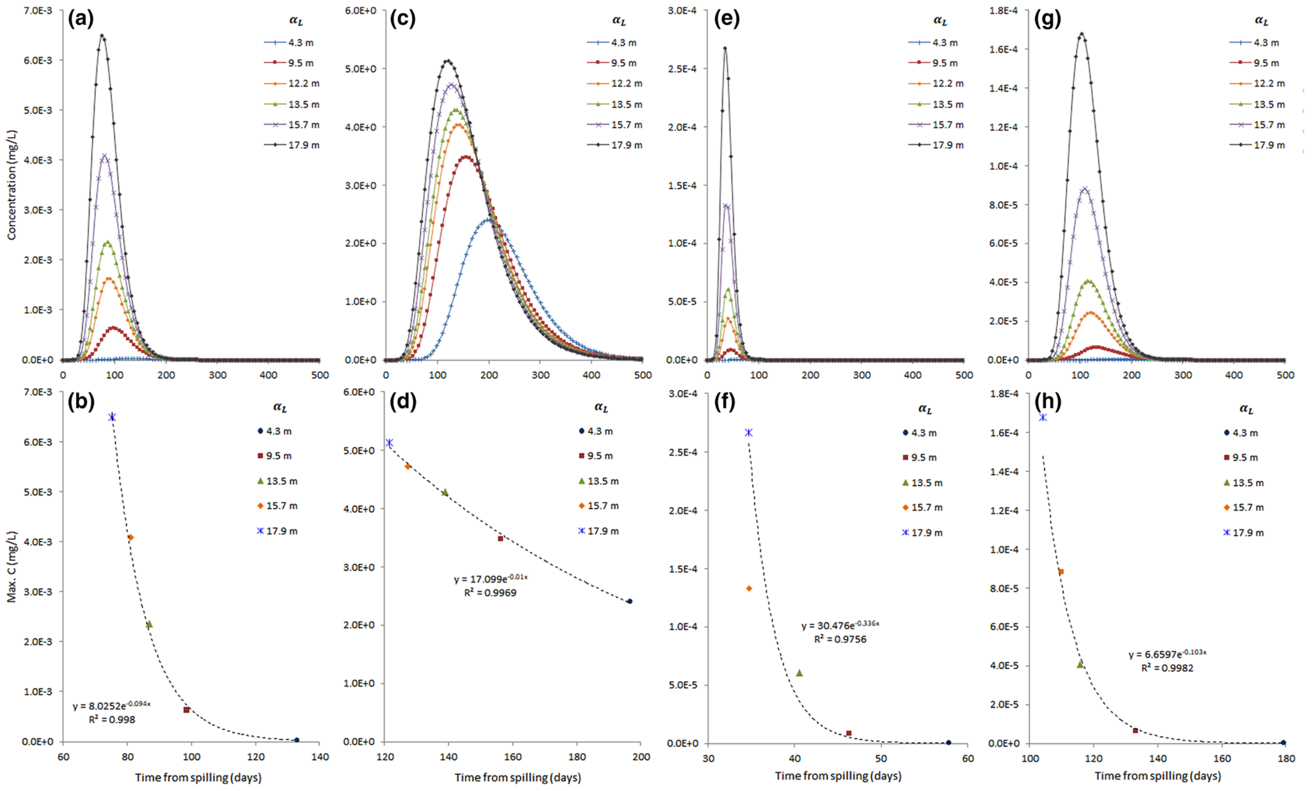

Fig. 10 Breakthrough curves for scenario 2: different values of α_L; $\alpha_T = 0.1\alpha_L$ (above) and maximum concentration of contaminant versus time from spilling (below). **a**, **b** Ametryn, **c**, **d** atrazine, **e**, **f** carbofuran, **g**, **h** diuron

a steady behavior for all other pesticides, i.e., the higher the ratio, the broader the contaminant plume in the direction perpendicular to the flow.

Scenario 4 The results from the simulations of scenario 4 for all four pesticides are shown in Fig. 13. As expected, the concentration of contaminants reaching the pumping well BR3 was higher as no degradation was taken into account. For carbofuran and diuron, such increment in the concentration was as high as four orders of magnitude, whereas for atrazine only one order of magnitude. This behavior is in concordance with the values of μ found with inverse modeling, i.e., the higher the value of μ, the higher the increment in concentration when no degradation is considered in the simulation.

Another effect is the difference shape of the BTCs. For all contaminants, the BTCs are a lot wider when no degradation is simulated and displaced to the right, which means that the contaminants persist in the aquifer for a longer time. The maximum concentrations reach the well BR3 much later when degradation is considered, and the order of their arrival coincides with the values of the retardation factor, R, found with the CXTFIT. Thus, the center of mass of diuron, which is the compound with a higher R (=4.2), is the last one to arrive at the well, whereas the one for carbofuran (R = 1.4) is the first one.

As the degradation constant affects the fate of the contaminants in the aquifer in such a manner, a more precise value of this parameter is needed when determining the fraction of μ (found with CXTFIT) that belongs to the dissolved and the sorbed phases.

Conclusions

The potential of riverbank filtration in the removal of organic compounds, most specifically pesticides, was approached from the stand point of laboratory column experiments and solute transport modeling. The chosen contaminants (ametryn, atrazine, carbofuran, diuron, and propanil) are of common use in Colombia, even though in Europe and the USA have been banned.

In total, six column experiments were performed at two different temperatures (10 °C and 20 °C) during an average

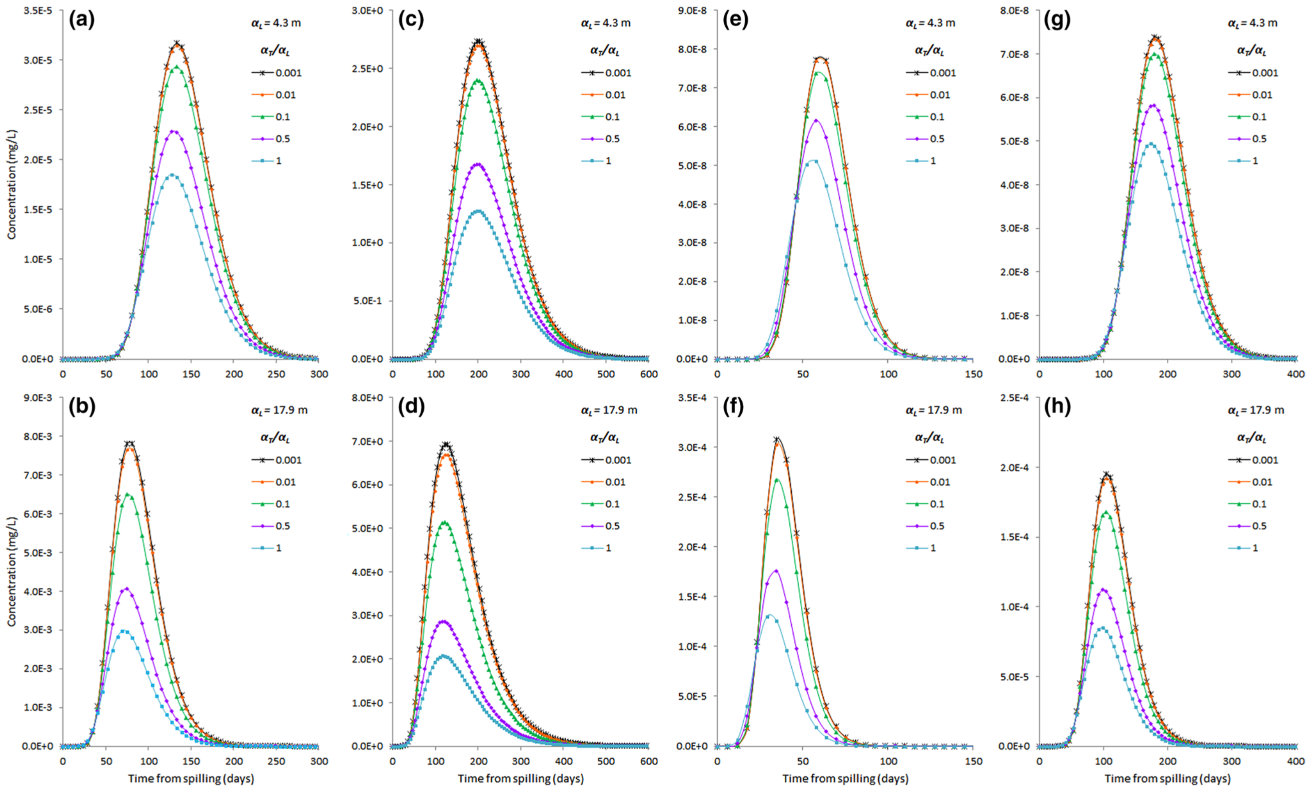

Fig. 11 Maximum concentration of the contaminants for scenario 3 with different values of α_T/α_L and α_L. **a**, **b** Ametryn, **c**, **d** atrazine, **e**, **f** carbofuran, **g**, **h** diuron

of 198 h per experiment. The maximum average removal was achieved for diuron, followed by carbofuran, ametryn, and atrazine. In the case of propanil, it rapidly transformed into the metabolite 3,4-dichloroaniline and was almost completely missing in the water samples, both from the inlet and the outlet.

The results of the laboratory experiments were used to find, through inverse modeling, transport parameters such as retardation factor, first-order degradation coefficient, and dispersion coefficient for each pesticide. The highest values of dispersion coefficient and retardation factor were those of diuron, whereas the lowest were the ones for carbofuran. Therefore, diuron was the contaminant that remained the longest in the soil and carbofuran was the one that travelled fastest. When it came to the first-order degradation coefficient, the highest values were for carbofuran, and the lowest for atrazine, which can be considered almost as a conservative tracer.

In order to simulate the effect of advection, dispersion, and degradation on the transport and fate of the contaminants, excluding propanil, a simulation with MT3DMS was implemented considering a hypothetical case of an accidental spill on the river. Additionally, the influence of degradation and the scale effect of dispersion due to flow length were evaluated with four different scenarios.

The results of the numerical model for the first three scenarios (where degradation was considered) showed a strong reduction in the highest concentration reaching the pumping well at the end of the simulation period compared to the initial concentration in the river. If no degradation was considered, the maximum concentrations at the well were 1–4 orders of magnitude higher than if degradation was taken into account. The differences in removal obtained during the column experiments and with the numerical modeling stress the importance of the length of the scale effect of the dispersion coefficient due to the length of the flowpath.

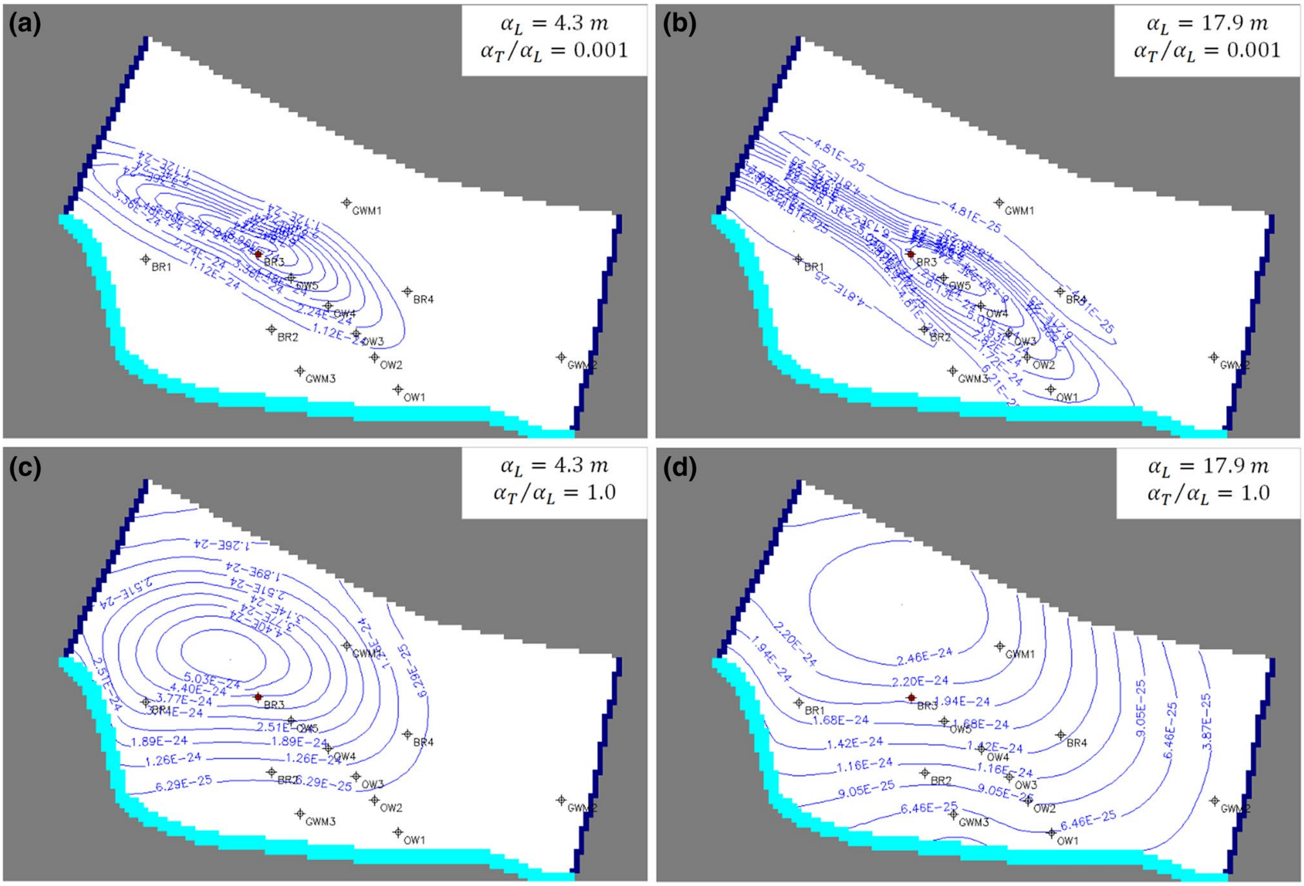

Fig. 12 Contaminant plumes for scenario 3 for ametryn at $\alpha_L = 4.3$ m (**a**, **b**), and $\alpha_L = 17.9$ m (**c**, **d**)

The results strongly support the advantage of mixing and dispersion during riverbank filtration offering a high safety against spills in a river. Under the given site conditions, and compared to the initial concentration in the river, the maximum pesticide concentrations, if only adsorption was considered, varied from 0.07% for diuron to 0.21% for carbofuran, but if both adsorption and degradation were simulated, the maximum concentration reaching the pumping well was 0.013% for atrazine. If the river water pollution by pesticides is lasting a few weeks, e.g., during a period of intensive application in agriculture, the buffering effect of riverbank filtration is lower, depending on average travel times, sorption, and degradation of the relevant compounds. In such cases, additional post-treatment may be required to provide safe drinking water.

The proven effects of dispersivity and degradation in the fate of contaminants in the subsoil underline the need to conduct laboratory and field experiments to determine reliable values for longitudinal and transverse dispersivity, as well as the fraction of the first-order degradation coefficients that belong to the dissolved and sorbed phases. Furthermore, the possible transformation of the considered solutes into metabolites should be assessed, because these could be more persistent and, therefore, pose a higher risk to drinking water supply than their parental compounds.

The results obtained in this work strengthen the hypothesis of the potential of RBF in reducing the concentration of agrochemicals and to counteract for peaks of contamination in the river even if no complete removal is achieved. However, for the same hydrogeological setting, the persistence of pesticides is not constant but varies depending on the properties of each compound.

The application of riverbank filtration in Colombia, where the pesticides studied in this project are still in use, could represent an alternative in water treatment for that percentage of the population who currently receives water that is not safe for human consumption. More research needs to be conducted in order to established the actual

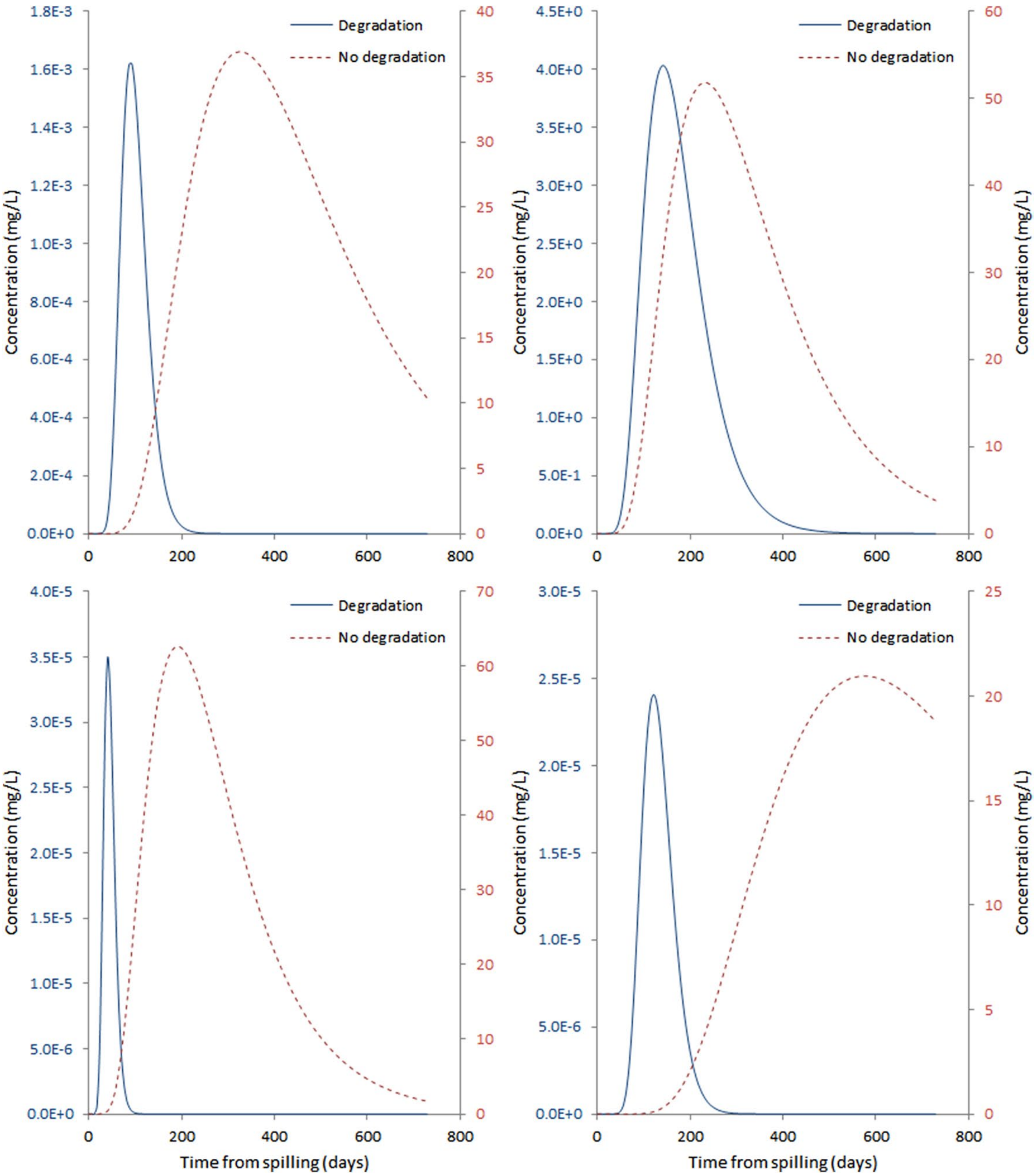

Fig. 13 Breakthrough curves for the contaminants for scenario 4, with degradation (solid line) and without degradation (discontinuous line), for $\alpha_L = 12.2$ m and $\alpha_T = 0.1\alpha_L$. **a** Ametryn, **b** atrazine, **c** carbofuran, **d** diuron

efficiency rate of RBF in the removal of pesticides in Colombian rivers, and to do so it would be interesting to consider the influence of climate in the process, either under normal hydrological conditions or during extreme precipitation events (like those occurring when La Niña conditions are being experimented) when runoff from the agricultural fields is expected to be higher.

Acknowledgements The authors thank the water company ZWA Hainichen for the field work support at the riverbank filtration site Loessnitztal in East Germany.

References

Agertved J, Rugge K, Barker JF (1993) Transformation of the herbicides MCPP and Atrazine under natural aquifer conditions. Groundwater 30(4):500–506

ASTM (2006) Standard practice for classification of soils for engineering purposes (unified soil classification system). Designation: D 2487-06. ASTM International, p 12

Baluch HU, Somasundaram L, Kanwar RS, Coats JR (1993) Fate of major degradation products of atrazine in Iowa soils. J Environ Sci Health B28(2):127–149

Benotti MJ, Song RG, Wilson D, Snyder SA (2012) Removal of pharmaceuticals and endocrine disrupting compounds through pilot- and full-scale riverbank filtration. Water Sci Technol Water Supply 12(1):11–23

Bertelkamp C, Reungoat J, Cornelissen ER, Singhal N, Reynisson J, Cabo AJ, van der Hoek JP, Verliefde ARD (2014) Sorption and biodegradation of organic micropollutants during river bank filtration: a laboratory column study. Water Res 52:231–241

Bertelkamp C, Verliefde ARD, Schoutteten K, Vanhaecke L, Vanden Bussche J, Singhal N, van der Hoek JP (2016) The effect of redox conditions and adaptation time on organic micropollutant removal during river bank filtration: a laboratory-scale column study. Sci Total Environ 544:309–318

Buchanan I, Liang HC, Liu Z, Razaviarani V, Rahman MdZ (2010) Pesticides and herbicides. Water Environ Res 82(10):1594–1693

Chiang W-H (2005) 3D-groundwater modeling with PMWIN: a simulation system for modeling groundwater flow and transport processes, 2nd edn. Springer, Berlin, p 414

Chiang W-H, Kinzelbach W (1994) PMPATH :an advective transport model for processing modflow and modflow. Geol Surv Hambg, Germany

Chiang W-H, Kinzelbach W (1998) Processing modflow: a simulation system for modeling groundwater flow and pollution. User's guide, p 334

Defensoria del Pueblo (2010) Diagnóstico de la calidad de agua para consumo humano año 2009, p 66

Defensoría del Pueblo (2007) Tercer diagnóstico sobre calidad de agua para consumo humano, p 168

DIN (2011) DIN 18123:2011-04-Baugrund, Untersuchung von Bodenproben-Bestimmung der Korngrößenverteilung (grain size distribution). Deutsches Institute fur Normung

Doussan C, Poitevin G, Ledoux E, Detay M (1997) River bank filtration: modelling of the changes in water chemistry with emphasis in nitrogen species. J Contam Hydrogeol 25:129–156

HTW Dresden (2012) Uferfiltration im Lößnitztal - Modellierung der Grundwasserströmung (Bank filtration at Loessnitztal: groundwater flow modeling). University of Applied Sciences Dresden, unpublished report, p 27

Eckhard W (1999) Laboratory tests for simulation of riverbank filtration processes. In: Abstracts international riverbank filtration conference, Louisville (Kentucky), November 4th–6th 1999, p 11

Fetter CW (1999) Contaminant hydrogeology, 2nd edn. Prentice Hall, Englewook Cliffs, p 500

Freeze RA, Cherry JA (1979) Groundwater. Prentice Hall, Englewook Cliffs, p 604

Fried JJ (1975) Groundwater pollution. Elsevier, Amsterdam, p 329

Hiscock KM, Grischek T (2002) Attenuation of groundwater pollution by bank filtration. J Hydrol 266(3–4):139–144

IAvH, IDEAM, IIAP, INVEMAR, SINCHI (2011) Informe del Estado del Medio Ambiente y de los Recursos Naturales Renovables 2010. Instituto de Hidrología, Meteorología y Estudios Ambientales–IDEAM, Bogotá, p 384

ICA (2011) Estadísticas de comercialización de plaguicidas químicos de uso agrícola 2010. Instituto Colombiano Agropecuario, Bogotá, p 96

ICA (2016) Estadísticas de comercialización de plaguicidas químicos de uso agrícola 2015. Instituto Colombiano Agropecuario, Bogotá, p 128

IDEAM (2010) Estudio Nacional del Agua 2010. Instituto de Hidrología, Meteorología y Estudios Ambientales, Bogotá, p 420

IDEAM (2015) Estudio Nacional del Agua 2014. Instituto de Hidrología, Meteorología y Estudios Ambientales, Bogotá, p 493

Jaramillo M (2012) Riverbank filtration: an efficient and economical drinking-water treatment technology. Dyna 171:148–157

Jekel M, Grischek T (2003) Riverbank filtration: the European experience. In: Melin G (ed) Riverbank filtration: the future is now. Program and abstracts of the 2nd international Riverbank Filtration conference, Cincinnati, Ohio, USA. September 16th–19th, 2003

Kuehn W, Mueller U (2000) Riverbank filtration: an overview. J Am Water Works Assoc (AWWA) 92(12):60–69

Kuster M, Díaz-Cruz S, Rosell M, López de Alda M, Barceló D (2010) Fate of selected pesticides, estrogens, progestogens and volatile organic compounds during artificial aquifer recharge using surface waters. Chemosphere 79:880–886

Lallemand-Barres P, Peaudecerf P (1978) Recherche des relations entre la veleur de la dispersivite macroscopique d'un milieu aquifere, ses autres caracteristiques et les conditions de mesure, etude bibliographique. Bulletin, Bureau de Recherches Geologiques et Miniéres, Sec. 3/4:277–287

Lewis J, Sjöstrom J (2010) Optimizing the experimental design of soil columns in saturated and unsaturated transport experiments. J Contam Hydrol 115:1–13

Mao M, Ren L (2005) Simulating nonequilibrium transport of Atrazine through saturated soil. Groundwater 42(4):500–508

Marquardt DW (1963) An algorithm for least-squares estimation of nonlinear parameters. J Soc Ind Appl Math 2:431–441

McDonald MG, Harbaugh AW (1988) A modular three-dimensional finite-difference ground-water flow model. U.S. Geological Survey, Techniques of water-resources investigations, book 6, chapter A1, p 586

Neuman SP (1990) Universal scaling of hydraulic conductivities and dispersivities in geologic media. Water Resour Res 26(8):1749–1758

Ormad MP, Miguel N, Claver J, Matesanz JM, Ovelleiro JL (2008) Pesticides removal in the process of drinking water production. Chemosphere 71:97–106

Pang L, Close ME (1999) Attenuation and transport of atrazine and picloram in an alluvial gravel aquifer: a tracer test and batch study. NZ J Mar Freshw Res 33(2):279–291

Paraiba LC, Spadotto CA (2002) Soil temperature effect in calculating attenuation and retardation factors. Chemosphere 48:905–912

Perkins TK, Johnson OC (1963) A review of diffusion and dispersion in porous media. Soc Petrol Eng J 3:70–84

Rashid B, Husnain T, Riazuddin S (2010) Herbicides and pesticides as potential pollutants: a global problem. In: Ashraf M et al (eds) Plant adaptation and phytoremediation. Springer, Berlin, pp 427–447

Ray C, Soong TWD, Roadcap GS, Borah DK (1998) Agricultural chemicals: effects on wells during floods. J Am Water Work Assoc 90:90–100

Ray C, Soong TW, Lian YQ, Roadcap GS (2002) Effect of flood-induced chemical load on filtrate quality at bank filtration sites. J Hydrol 266:235–258

Romero LG, Pizzolati BS, Soares MBD, Michelan DCGS, Sens ML (2010) Bank filtration: application in rural areas. Case studies in Santa Catarina, Brazil. In: Conference proceedings on 21st century watershed technology: improving water quality and environment

SAN (2011) List of prohibited pesticides. Sustainable agriculture network, p 8

Sánchez-Pérez JM, Montuelle B, Mouchet F, Gauthier L, Julien F, Sauvage S, Teissier S, Dedieu K, Destrieux D, Vervier P, Gerino M (2013) Role of the hyporheic heterotrophic biofilm on transformation and toxicity of pesticides. Ann Limnol Int J Lim 49:87–95

Schaffner C, Ahel M, Giger W (1987) Field studies on the behaviour of organic micropollutants during infiltration of river water to groundwater. Water Sci Technol 19:1195–1196

Scribner EA, Thurman EM, Zimmerman LR (2000) Analysis of selected metabolites in surface and ground water in the United States. Sci Total Environ 248:157–167

Simunek J, van Genuchten MTh, Sejna M, Toride N, Leij FJ (1999) The STANMOD computer software for evaluating solute transport in porous media using analytical solutions of convection-dispersion equation. Versions 1.0 and 2.0, IGWMC-TPS-71. International Ground Water Modeling Center, Colorado School of Mines, Golden, Colorado, p 32

Sinclair CJ, Boxall ABA (2003) Assessing the ecotoxicity of pesticide transformation products. Environ Sci Technol 37(20):4617–4625

Son BT (2010) Role of riverbank filtration in the attenuation of herbicides. Ph.D. Dissertation, School of Environmental Sciences, University of East Anglia, p 255

Toride N, Leij FJ, van Genuchten MTh (1995) The CXTFIT code for estimating transport parameters from laboratory or field tracer experiments, version 2.0, research report no. 137. U. S. Salinity Laboratory, USDA, ARS, Riverside, CA, p 131

Tufenkji N, Ryan JN, Elimelech M (2002) The promise of bank filtration. Environ Sci Technol 1:423–428

University of Hertfordshire's PPDB (pesticide properties database). http://sitem.herts.ac.uk/aeru/ppdb/en/index.htm. Cited 3 Aug 2014

U.S. National Library of Medicine's TOXNET system. http://toxnet.nlm.nih.gov. Cited 15 Nov 2014

Verstraeten IM, Heberer T (2002) Organic chemical removal issues. In: Ray C, Melin G, Linsky R (eds) Riverbank filtration improving source-water quality, vol 43. Springer, Berlin, pp 321–330

Verstraeten IM, Carr JD, Steele GV, Thurman EM, Dormedy DF (1999) Surface-water/ground-water interaction: herbicide transport into municipal collector wells. J Environ Qual 28(5):1396–1405

Verstraeten IM, Heberer T, Scheytt T (2002a) Occurrence, characteristics, transport, and fate of pesticides, pharmaceuticals, industrial products, and personal care products at riverbank filtration sites. In: Ray C, Melin G, Linsky R (eds) Riverbank filtration improving source-water quality, vol 43. Springer, Berlin, pp 175–227

Verstraeten IM, Thurman EM, Lindsey ME, Lee EC, Smith RE (2002b) Changes in concentrations of triazine and acetamide herbicides by bank filtration, ozonation, and chlorination in a public water supply. J Hydrol 266:190–208

Xu M, Eckstein Y (1995) Use of weighted least-squares method in evaluation of the relationship between dispersivity and field scale. Ground Water 16(6):905–908

Zheng C, Wang P (1999) MT3DMS A modular three-dimensional multispecies transport model for simulation of advection, dispersion and chemical reactions of contaminants in groundwater systems: documentation and user's guide. US Army Corps of Engineers, Washington, DC, p 239